Blinking in quantum dots: The origin of the grey state and power law statistics

Mao Ye[1] and Peter C. Searson[1,2,*]

[1]*Department of Materials Science and Engineering, and Department of Physics and Astronomy, Johns Hopkins University, Baltimore, Maryland 21218, USA*

[2]*Institute for Nanobiotechnology (INBT), Johns Hopkins University, Baltimore, Maryland 21218, USA*

Quantum dot (QD) blinking is characterized by switching between an "on" state and an "off" state, and a power-law distribution of on and off times with exponents from 1.0 to 2.0. The origin of blinking behavior in QDs, however, has remained a mystery. Here we describe an energy-band model for QDs that captures the full range of blinking behavior reported in the literature and provides new insight into features such as the gray state, the power-law distribution of on and off times, and the power-law exponents.

Semiconductor quantum dots (QDs) represent one of many systems that exhibit intermittent fluorescence, or blinking, characterized by switching between an "on" state and an "off" state. The on and off times span a broad range, typically from milliseconds to minutes, and exhibit power-law behavior ($f = B\tau^{-\alpha}$) with exponents (α) between 1.0 and 2.0. In some cases, switching may occur between an on state and a low-intensity or "gray" state. The origin of the blinking behavior in QDs, however, has "remained a mystery."[1]

In 1997 Efros and Rosen[2] proposed the most cited model for QD blinking.[3] In this four-state model based on semiconductor physics, a QD (state 1) can absorb a photon generating an electron-hole pair (state 2). Radiative band-to-band recombination results in emission of a photon (and return to state 1), whereas absorption of a second photon, before recombination of the electron-hole pair, leads to the creation of two electron-hole pairs (state 3). There are two possible pathways from this state: (1) radiative band-to-band recombination (return to state 2), and (2) nonradiative Auger recombination with simultaneous excitation of an electron to a trap state, resulting in a valence band hole and a trapped electron (state 4). The trapped electron is assumed to have very slow detrapping kinetics resulting in the off state. Auger recombination is an intra-QD energy transfer interaction in which the excess energy from a band-to-band recombination event is transferred to a spectator charge carrier rather than emitted as a photon.

While various modifications to the Efros-Rosen model have been suggested, and other statistical models have been proposed to explain the power-law behavior,[1,4–6] the physics of the blinking behavior remains unresolved.[1,7,8] Here we describe an energy-band model for QDs that captures the range of blinking behavior reported in the literature and provides insight into features such as the gray state, the power-law distribution of on and off times, and the power-law exponents.

I. MODEL IMPLEMENTATION

A. Intensity-time curves

Figure 1 shows energy-band diagrams for the various states in our model, along with the associated rate constants. Our model is implemented using standard kinetic Monte Carlo methods (KMC)[9] and is based on the physics of QDs[10–12] combined with descriptions for recombination and trapping processes widely used in device physics (Table I). We denote each state in the QD as (ij), where i is the total number of electrons (holes) in the QD, and j is the number of trapped charge carriers. Without losing any generality, we assume that only electrons can be trapped. From examination of Fig. 1 it is evident that $p = i$, $n = i - j$, and $s^- = j$, where n is the number of free electrons, p is the number of free holes, and s^- is the number of occupied trap states.

For each state (ij) there are several possible transitions to adjacent states, and these transitions have corresponding rates $r_1, r_2, \ldots r_n$. The time that a QD will remain in a certain state is given by $\Delta t = -\ln R/\sum r_i$, where R is a random number between 0 and 1. The probability that a QD will move to a particular state is given by $r_i/\sum r_i$. A QD with no electrons or holes is designated as in the (00) state ($n = 0$, $p = 0$, $s^- = 0$). Absorption of a photon and the generation of an e-h pair results in a transition to the (10) state ($n = 1$, $p = 1$, $s^- = 0$). From the (10) state, there are three possible transitions, indicated by the arrows in Fig. 1: (1) radiative recombination (k_r) returns the QD to the (00) state with the emission of a photon, (2) trapping of the electron (k_t) results in a transition to the (11) state ($n = 0$, $p = 1$, $s^- = 1$), and (3) absorption of another photon (g) results in a transition to the (20) state ($n = 2$, $p = 2$, $s^- = 0$).

The transition from the (10) state is determined from the sum of all possible rates ($r_r + r_t + g$), as described above. For the (10) state, the residence time is given by $\Delta t = -\ln R/(r_r + r_t + g)$. We then subdivide the range from 0 to 1 into three parts, each with a length the same as the probability of each transition. For example, the probability of the transition from the (10) state to the (00) state is determined by $r_r/(r_r + r_t + g)$. The transition is then selected by generating another random number between 0 and 1. Since k_r is typically much larger than g and k_t, there is a high probability that the QD will relax from the (10) state to the (00) state. Oscillation between the (00) and (10) states represents sequential absorption and emission in the QD. Population of the (20) state gives rise to the possibility of Auger recombination, which is usually considered to be faster than radiative recombination. For all transitions between (i0) states, the QD is considered to be in the on state and no blinking is observed. Even though Auger recombination (k_A) may dominate in (i0) states with $i \geqslant 2$, we consider these configurations as on states as they return to the (00) state with high probability.
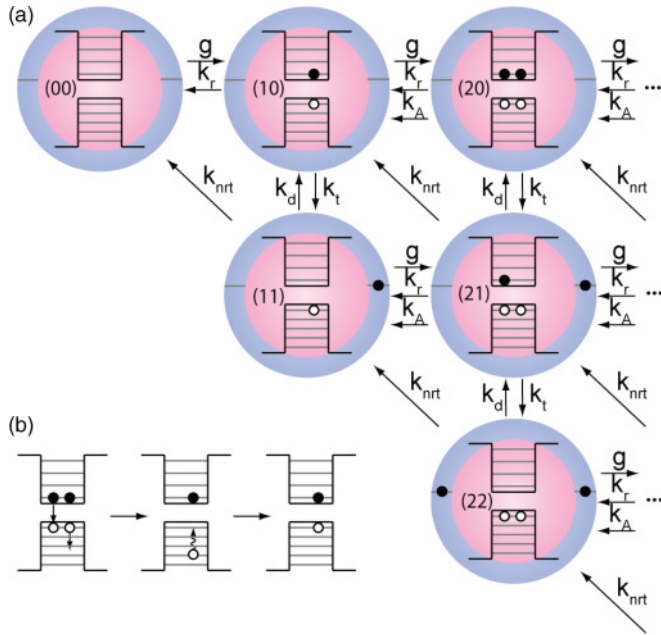
FIG. 1. (Color) Energy-band diagrams illustrating the dynamics of electron-hole pairs in blinking quantum dots. (a) Physical processes in quantum dot blinking: g:generation rate, k_r: recombination rate constant, k_A: rate constant for Auger recombination, k_t: trapping rate constant, k_d: detrapping rate constant, k_{nrt}: rate constant for nonradiative recombination. (b) Auger recombination in quantum dots. Band-to-band recombination is coupled with excitation of a charge carrier (in this case a hole) that quickly relaxes (on the order of picoseconds) back to the band edge.

The population of states with trapped carriers ($j \geqslant 1$) results in off states. For example, consider the (21) state ($n = 1, p = 2$, $s^- = 1$), for which there are six possible transitions: (1) return to the (20) state by detrapping (k_d), (2) transition to the (10) state by nonradiative recombination involving the trap state (k_{nrt}), (3) transition to the (31) state by absorption of a photon and generation of an e-h pair (g), (4) transition to the (11) state by radiative recombination and generation of a photon (k_r), (5) transition to the (11) state by Auger recombination (k_A), and (6) transition to the (22) state by trapping the conduction band electron (k_t).

From Fig. 1 it is evident that if $k_A > k_r$ (and $k_A > k_t, k_d$, k_{nrt}) then the QD will remain in the off state since e-h pair generation will most likely be followed by a return to the same state through nonradiative Auger recombination (k_A). Detrapping (k_d) and nonradiative recombination via trap states (k_{nrt}) both return the QD to the on state. Switching between the on and off states that leads to blinking is controlled by k_t, k_d, and k_{nrt} which are generally much slower than g, k_r, and k_A. The intensity-time curves are obtained by counting the number of photons emitted in each bin (integration) time (I_n).

B. On-time fraction (P_{on})

To characterize the blinking behavior for a given set of rate constants, we first write the system of rate equations corresponding to the processes indicated in Fig. 1. We denote the probability of finding a QD in a given state by P_{ij}. For example, the (00) state can be accessed from the (10) state by radiative recombination (k_r), or from the (11) state by nonradiative recombination via trap states (k_{nrt}). In addition, the (00) state can transition to the (10) state by generation of an e-h pair (g) which would decrease the probability of finding a QD in the (00) state. Thus, the time-dependent probability for the (00) state is given by

$$\frac{dP_{00}}{dt} = k_r P_{10} + k_{nrt} P_{11} - g P_{00}. \tag{1}$$

As an example, the system of equations for a maximum of 2 e-h pairs is

$$\frac{dP_{00}}{dt} = k_r P_{10} + k_{nrt} P_{11} - g P_{00}, \tag{2}$$

$$\frac{dP_{10}}{dt} = g P_{00} + k_d P_{11} + 1 \cdot 2k_{nrt} P_{21} + (2 \cdot 2k_r + 2 \cdot 2^2 k_A) P_{20} - (k_r + sk_t + g) P_{10}, \tag{3}$$

$$\frac{dP_{20}}{dt} = g P_{10} + k_d P_{21} - (2 \cdot 2k_r + 2 \cdot 2^2 k_A + 2sk_t) P_{20}, \tag{4}$$

$$\frac{dP_{11}}{dt} = sk_t P_{10} + 2 \cdot 2k_{nrt} P_{22} + (1 \cdot 2k_r + 1 \cdot 2^2 k_A) P_{21} - (k_d + k_{nrt} + g) P_{11}, \tag{5}$$

TABLE I. Summary of processes included in the model and the corresponding rate equations.

Process	Rate equation	
Radiative recombination	$r_r = k_r np$	k_r: rate constant for radiative recombination
		n: number of electrons
		p: number of holes
Auger recombination	$r_A = k_A np^2$	k_A: rate constant for Auger recombination
Trapping	$r_t = k_t ns^0$	k_t: rate constant for trapping
		s: total number of trap states ($s = s^0 + s^-$)
		s^0: number of empty trap states
		s^-: number of occupied trap states
		Note: We arbitrarily choose $s = s^- + s^0 = 10$
Detrapping	$r_d = k_d s^-$	k_d: rate constant for detrapping
Nonradiative recombination	$r_{nrt} = k_{nrt} s^- p$	k_{nrt}: rate constant for nonradiative recombination

$$\frac{dP_{21}}{dt} = 2sk_t P_{20} + g P_{11} + 2k_d P_{22} - [k_d + 2k_{nrt} + 2k_r$$
$$+ 1 \cdot 2^2 k_A + 1 \cdot (s-1)k_t]P_{21}, \qquad (6)$$

$$\frac{dP_{22}}{dt} = 1 \cdot (s-1)k_t P_{21} - (2 \cdot 2k_{nrt} - 2k_d)P_{22}. \qquad (7)$$

The equations can be solved for different values of the rate constants by recognizing that in steady state $dP_{ij}/dt = 0$ and that $\Sigma P_{ij} = 1$. The on-time fraction P_{on} is given by

$$P_{on} = \sum P_{i0}. \qquad (8)$$

The off-time fraction P_{off} is given by

$$P_{off} = \sum_{j \geqslant 1} P_{ij}. \qquad (9)$$

Experimentally, P_{on} is usually obtained by defining a threshold (I_{th}) between the on and off intensities (I_{on} and I_{off}). This procedure may introduce artifacts; however, as long as the on and off intensities are well separated then P_{on} is the same for both methods.

C. Distributions of on and off times

Intensity distributions were obtained from intensity-time curves. To obtain the on and off times, we first determined the threshold intensity I_{th} from the intensity distribution. Gaussians were fit to the on and off peaks and I_{th} was obtained from the intersection point between the two peaks. The QD was considered to be "on" when $I_n \geqslant I_{th}$, and "off" when $I_n < I_{th}$. If I_n remains above or below I_{th} for i sequential time bins, then $\tau_{i,on/off} = i\tau_{bin}$. The intensity-time curve is thus converted to a sequence of on and off times. We then create a histogram describing the number of occurrences N_i of each duration τ_i ($1 \leqslant i \leqslant M$). The shortest duration (τ_1) is limited by the bin time (τ_{bin}), while the longest duration (τ_M) is limited by the total time (τ_{total}). Total number of occurrences of on or off times is

$$N^{total} = \sum_{1 \leqslant i \leqslant M} N_i. \qquad (10)$$

The distribution of on and off times, or formally, the probability density f_i, is given by

$$f_i = \frac{N_i/N^{total}}{[(\tau_{i+1} - \tau_i) + (\tau_i - \tau_{i-1})]/2}, \qquad (11)$$

where $2 \leqslant i \leqslant M-1$. At the limits ($i = 1$ and $i = M$) we set $\tau_0 = \tau_1$ and $\tau_{M+1} = \tau_M$. The power-law exponents ($\alpha_{on/off}$) or exponential times ($\tau_{0,on/off}$) are determined from a least-squares fit of the $\log(f_{i,on/off})$ versus $\log(\tau_{i,on/off})$ curves.

D. Quantum yield

The on and off quantum yields were calculated by averaging all the intensities above or below the threshold over time divided by the number of photogenerated electron-hole pairs:

$$QY_{on} = \frac{\sum_{I_n > I_{th}} I_n}{\sum g_n}, \qquad (12)$$

$$QY_{off} = \frac{\sum_{I_n < I_{th}} I_n}{\sum g_n}. \qquad (13)$$

Experimentally, evaluation of QY_{on} and QY_{off} requires careful analysis of the distribution of intensities from intensity-time curves. If the intensities associated with the on and off states are well separated then it is trivial to set an appropriate threshold. However, if the distributions of on and off intensities overlap, then distinguishing between on and off states is more difficult. This can often be accomplished by fitting two Gaussians to the distribution, one representing the on state and one representing the off state.

E. Generation

The generation rate g (ms^{-1}) in a spherical QD with absorption coefficient α (cm^{-1}) is given by

$$g = \frac{I_0 \pi d^2}{4h\nu}\left[1 - 2\frac{1 - (1 + \alpha d)e^{-\alpha d}}{(\alpha d)^2}\right], \qquad (14)$$

where I_0 is the incident power density (W cm^{-2}), $h\nu$ is the photon energy, and d is the QD diameter. We assume that the absorption coefficient for a nanoparticle is the same as for a bulk material.

Absorption can also be defined in terms of the absorption cross section σ:

$$\sigma = \frac{\pi d^2}{4}\left[1 - 2\frac{1 - (1 + \alpha d)e^{-\alpha d}}{(\alpha d)^2}\right], \qquad (15)$$

such that $g = I_0\sigma/h\nu$.

For a 5-nm-diam CdSe QD, taking an absorption coefficient $\alpha = 10^5$ cm^{-1} at $\lambda = 400$ nm (Ref. 13) and an incident power density of 0.1–1000 W cm^{-2} (Refs. 14–16), the generation rate g is typically in the range 1–10^4 ms^{-1}.

The generation rate is linearly dependent on incident power density, QD volume, and absorption coefficient.[3] The bulk absorption coefficient for most semiconductors of interest is in the range from 10^5 to 10^6 cm^{-1}. The QD diameter is typically 3–10 nm, corresponding to an order-of-magnitude range of volume. Although the range of power density may be quite large, experimentally, the power density is adjusted so that the emission from the QD does not saturate the detector using an exposure time of around 10 ms.

F. Trapping and detrapping

Radiative band-to-band recombination is expected to be fast with a rate constant $k_r = 10^3$–10^6 ms^{-1} (Table II).[17–21] If there are more than two free carriers in a QD, Auger recombination [Fig. 1(b)] is expected to be dominant with a rate constant $k_A = 10^5$–10^8 ms^{-1} (Refs. 22–27).

It is evident from examination of an energy-band diagram (Fig. 1) that trapping, detrapping, and Auger recombination are essential to create configurations where blinking is observed. In configurations where trap states are occupied ($j \geqslant 1$), electron-hole pairs are eliminated primarily by Auger recombination ($k_A > k_r$) and the QD is predominantly in an off state. Conversely, configurations where $j = 0$ can easily reach the (10) state where radiative recombination dominates. Thus configurations in the top row ($j = 0$) represent the on

TABLE II. Typical values of parameters used in the model.

Parameter	Typical values (ms^{-1})
k_r	10^3–10^6
k_A	10^5–10^8
g	1–10^3
Constant trapping and detrapping rates	
k_t	10^{-4}–10^2
$k_d + k_{nrt}$	10^{-3}–10^{-2}
Variable trapping and detrapping rates	
k_t	10^{-2}–10^2
$k_d + k_{nrt}$	10^{-5}–10^{-1}
$r_{t,eff}$	10^{-5}–10^{-1}
$r_{d,eff}$	10^{-5}–10^{-1}

state of a QD, and configurations below the top row ($j \geqslant 1$) correspond to the off state.

The rate of trapping is given by $r_t = k_t n s^0$ where n is the number of electrons in the QD and s^0 is the number of empty trap states. The detrapping rate is given by $r_d = k_d s^-$ where s^- is the number of occupied trap states. For all results reported here, we arbitrarily choose 10 trap states ($s = 10$), although as we show later, the steady-state number of trapped electrons is typically < 3.

Blinking requires switching between an on state ($i0$) and an off state (ij) where $j \geqslant 1$. The overall trapping and detrapping rates for a single QD, taking into account all configurations, can be described in terms of effective trapping and detrapping rates:

$$r_{t,\text{eff}} = \frac{\sum r_{t,i0} P_{i0}}{\sum P_{i0}} = \frac{s k_t \sum P_{i0}}{\sum P_{i0}}, \tag{16}$$

$$r_{d,\text{eff}} = \frac{\sum (r_{d,i1} + r_{\text{nrt},i1}) P_{i1}}{\sum_{j \geqslant 1} P_{ij}} = \frac{k_d \sum P_{i1} + k_{\text{nrt}} \sum i P_{i1}}{\sum_{j \geqslant 1} P_{ij}}, \tag{17}$$

where P_{ij} is the probability of state (ij). The blinking behavior can then be described in terms of the on-time fraction P_{on}, as a function of $r_{t,\text{eff}}$ and $r_{d,\text{eff}}$:

$$P_{\text{on}} = \frac{r_{d,\text{eff}}}{r_{t,\text{eff}} + r_{d,\text{eff}}}, \tag{18}$$

where $P_{\text{on}} = 1$ for a QD that is always on and $P_{\text{on}} < 1$ for blinking. To achieve the on and off times observed experimentally, typically in the range from 1 ms to 100 s, the effective trapping and detrapping rates should be on the order of 10^{-5}–10^0 ms^{-1}.

II. RESULTS AND DISCUSSION

Intensity-time curves from the model are able to reproduce the full range of behavior observed experimentally. Figure 2(a) shows a typical nonblinking luminescence curve. For an integration (bin) time of 10 ms, the distribution of on intensities shows a peak at around 100 photons, corresponding to a quantum yield of 1.0. Increasing $r_{t,\text{eff}}/r_{d,\text{eff}}$ to 10^{-1} by changing k_t results in blinking with $P_{\text{on}} = 0.91$ [Fig. 2(b)]. The average on intensity (I_{on}) remains 100 photons per bin
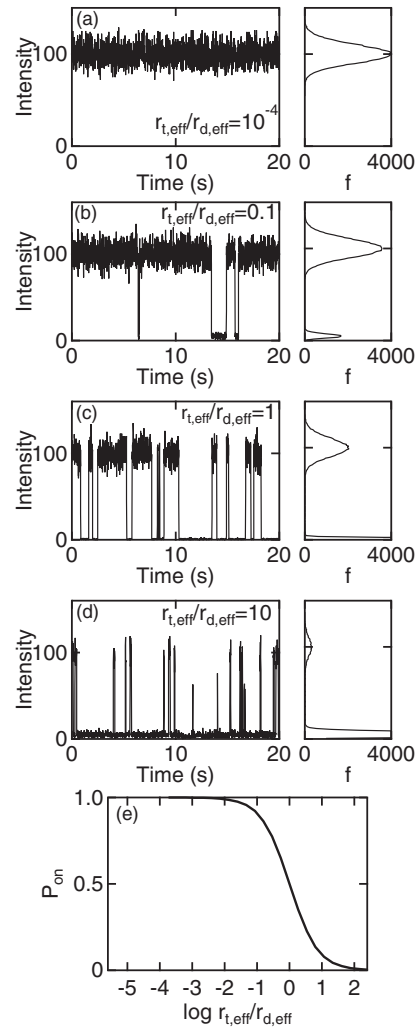

FIG. 2. Simulated intensity-time curves, and intensity distributions as a function of effective trapping-detrapping ratio $r_{t,\text{eff}}/r_{d,\text{eff}}$ with $k_d = 10^{-3}$ ms^{-1}, $k_{\text{nrt}} = 0$ ms^{-1}, $s = 10$, $k_r = 10^5$ ms^{-1}, $k_A = 10^7$ ms^{-1}, $g = 10$ ms^{-1}. (a) $r_{t,\text{eff}}/r_{d,\text{eff}} = 10^{-4}$ ($k_t = 10^{-4}$ ms^{-1}), (b) $r_{t,\text{eff}}/r_{d,\text{eff}} = 10^{-1}$ ($k_t = 10^{-1}$ ms^{-1}), (c) $r_{t,\text{eff}}/r_{d,\text{eff}} = 10^0$ ($k_t = 10^0$ ms^{-1}), (d) $r_{t,\text{eff}}/r_{d,\text{eff}} = 10$ ($k_t = 10$ ms^{-1}). In all cases the integration (bin) time was 10 ms, and (e) Dependence of P_{on} on the effective trapping/detrapping ratio $r_{t,eff}/r_{d,eff}$ showing that blinking occurs over a range of $r_{t,\text{eff}}/r_{d,\text{eff}}$ from 10^{-2} to 10^2.

(QY$_{\text{on}} = 1.0$) with a maximum frequency of 91% of the value for the corresponding nonblinking curve [Fig. 2(a)]. The off-intensity distribution is much narrower than the on-intensity distribution, and would only be observed experimentally if the fluctuations are larger than the noise of the photodetector. Increasing $r_{t,\text{eff}}/r_{d,\text{eff}}$ to 10^0 decreases P_{on} to 0.5 [Fig. 2(c)], and increasing $r_{t,\text{eff}}/r_{d,\text{eff}}$ further to 10^1 decreases P_{on} to 0.09 [Fig. 2(d)]. These results show that the blinking behavior is controlled by $r_{t,\text{eff}}/r_{d,\text{eff}}$.

Figure 2(e) shows that the blinking regime occurs over a range of $r_{t,\text{eff}}/r_{d,\text{eff}}$ from 10^{-2} to 10^2. To illustrate the relative importance of the parameters in the model, we consider a simple case involving the (00), (10), (11), (21) states. These are the four states most frequently occupied at low generation

rates. Taking into account the relevant rate constants, it is straightforward to show that

$$r_{t,\text{eff}} = \frac{s k_t g}{g + k_r}, \tag{19}$$

$$r_{d,\text{eff}} = \frac{(k_d + k_{\text{nrt}})(k_r + 2k_A)}{g + k_r + 2k_A}. \tag{20}$$

In most cases of experimental interest, $k_r > g$ and hence $r_{t,\text{eff}} \to s k_t g / k_r$. Similarly, it is also expected that $k_r + 2k_A > g$, so that $r_{d,\text{eff}} \to k_d + k_{\text{nrt}}$ and hence P_{on} is independent of k_A (at constant s, k_t, and $k_d + k_{\text{nrt}}$). Deviations from these approximations are observed at higher generation rates.

From Eq. (19) it is seen that increasing the generation rate results in an increase in $r_{t,\text{eff}}$ and hence is expected to decrease P_{on}. The generation rate is dependent on several parameters; however, for a given system it is very difficult to vary the generation rate over a wide range: the generation rate must be high enough so that the signal on the detector allows the on and off states to be clearly distinguished, but not too high to result in saturation.

The trapping and detrapping processes are controlled by k_t and $k_d + k_{\text{nrt}}$. k_t and k_d can be described by two possible mechanisms.[28] (1) Trapping and detrapping involve delocalized electrons and states at the core-shell interface. Energetically, the trap states are expected to be located in the band gap so that trapping is downhill and detrapping is thermally activated. (2) Trapping and detrapping occur by tunneling between delocalized electrons in the core to states in the shell or at the surface of the shell if it is sufficiently thin. Nonradiative recombination via trap states k_{nrt} contributes to blinking in the same way as k_d even though they represent different physical processes.[22] The expressions for k_t, k_d, and k_{nrt} are dependent on the mechanism but do not influence the results reported here.

A. Binning time and total time

The binning time, which is usually set by the minimum camera exposure time necessary to distinguish the QD from the background (typically in the range from 200 μs to 100 ms, but usually around 10 ms),[15,29,30] plays a key role in determining the blinking characteristics. If the effective trapping and detrapping rates, $r_{t,\text{eff}}$ and $r_{d,\text{eff}}$ are faster than $1/\tau_{\text{bin}}$, then switching is likely to occur in each frame and the QD will appear always on with an average intensity $I_{\text{av}} = I_{\text{max}} P_{\text{on}}$, where $I_{\text{max}} = g \tau_{\text{bin}}$. Conversely, if $r_{t,\text{eff}}$ and $r_{d,\text{eff}}$ are slower than $1/\tau_{\text{total}}$ (where τ_{total} is typically up to 1000 s), then there will be very few switching events in the intensity-time curves. Thus for blinking to occur, $r_{t,\text{eff}}$ and $r_{d,\text{eff}}$ must be $>1/\tau_{\text{total}}$ and $<1/\tau_{\text{bin}}$. Practically, this corresponds to a range from $\sim$10 ms to $\sim$100 s.

B. Gray state

Experimentally, intensity-time curves for QDs sometimes show an off state that is above the background signal of the detector, the so-called gray state.[14,25,31] Figure 3(a) shows an intensity-time curve where the parameters are the same as for Fig. 2(c), except that k_A is decreased from 10^7 ms^{-1} to 10^6 ms^{-1}. The intensity distribution [Fig. 3(a)] shows the
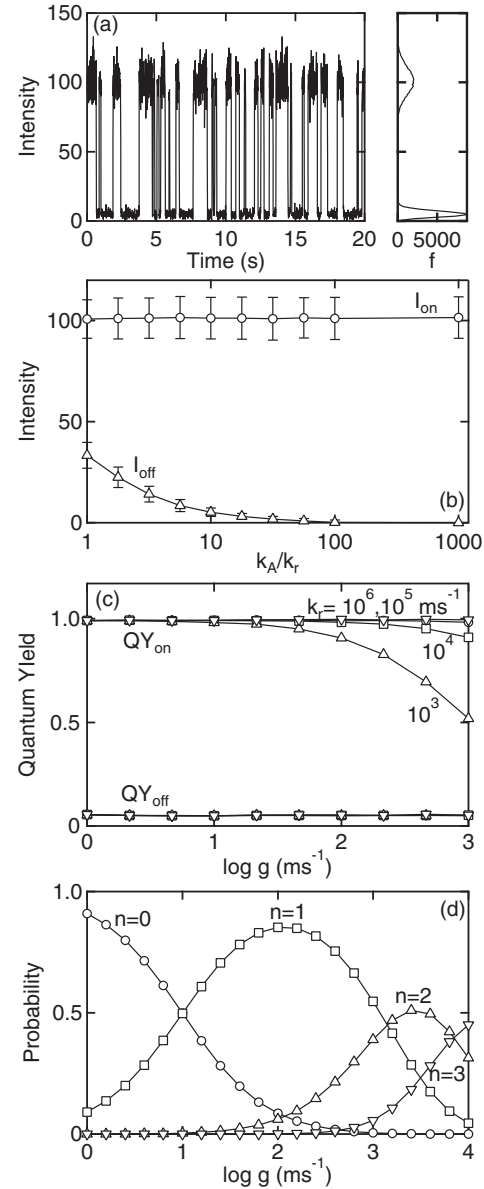

FIG. 3. Influence of important rate constants on the on and off intensities. (a) Intensity-time curve (photons/10 ms) and intensity distribution illustrating the gray state. The parameters are the same as for Fig. 2(c) except that k_A is decreased from 10^7 ms^{-1} to 10^6 ms^{-1}. Other parameters are $k_r = 10^5$ ms^{-1}, $g = 10$ ms^{-1}, $k_t = 10^0$ ms^{-1}, $k_d = 10^{-3}$ ms^{-1}, $k_{\text{nrt}} = 0$ ms^{-1}, and $s = 10$ with $r_{t,\text{eff}}/r_{d,\text{eff}} = 1$. (b) On and off intensities and their fluctuations versus k_A/k_r (1–10^3) with $k_r = 10^5$ ms^{-1}. Other parameters are the same as (a). (c) Quantum yield for on and off states versus generation rate g (1–10^3 ms^{-1}) at different radiative recombination rates ($k_r = 10^3$–10^6 ms^{-1}) with $k_A/k_r = 10$. Other parameters are: $s = 10$, $k_d = 10^{-3}$ ms^{-1}, $k_{\text{nrt}} = 0$ ms^{-1}, k_t chosen such that $r_{t,\text{eff}}/r_{d,\text{eff}} = 10^0$ and $P_{\text{on}} = 0.5$. (d) Probability of the steady-state number of electron-hole pairs versus generation rate ($g = 1$–10^3 ms^{-1}), with other parameters the same as in (a).

emergence of a gray state where the off-state distribution is shifted above zero.

The gray state is dependent primarily on k_A, k_r, and g. Figure 3(b) shows the magnitude of on and off intensities, as

well as the amplitude of their fluctuations, plotted versus k_A/k_r ($k_r = 10^5$ ms^{-1}). For a bin time of 10 ms, the on intensity is $\sim$100 photons/bin with fluctuations of $\sim$10 photons/bin, independent of k_A/k_r. In the off state, the radiative and Auger recombination pathways operate in parallel, and hence we have

$$QY_{off} = \frac{1}{1 + 2k_A/k_r}. \qquad (21)$$

Thus as $k_A \rightarrow k_r$, QY_{off} increases and reaches a value of 0.33 when $k_A = k_r$. Also note that when $QY_{on} = 1$ then $QY_{off} = I_{off}/I_{on}$.

When k_A/k_r is large, $I_{off}/I_{on} \rightarrow 0$, and the off state in an experiment would coincide with the background signal of the detector. In contrast, as $k_A \rightarrow k_r$, I_{off}/I_{on} becomes significant so that the off state can be resolved above the background signal of the detector. In all cases, the on and off intensities and their fluctuations are not significantly influenced by the trapping and detrapping rate constants.

The influence of g and k_r on the on and off quantum yields for a typical gray state is shown in Fig. 3(c). The ratio k_A/k_r is maintained constant and the trapping rate constant is tuned so that the on-time fraction is always around 0.5 (see Fig. 2). As previously described, k_t, k_d, and k_{nrt} only affect the on-time fraction. As the generation rate increases, QY_{off} remains approximately constant at around 0.05. In contrast, QY_{on} decreases above a characteristic value of g due to the presence of multiple e-h pairs (see next paragraph) and the increasing contribution of Auger recombination.[24,26,32] When $g \rightarrow k_r$, the probability of creating more than one e-h pair increases (see Fig. 1), and hence the contribution from Auger recombination results in a decrease in QY_{on}. For example, for $g = 10^3$ ms^{-1}, QY_{on} decreases from 0.98 when $k_r = 10^5$ ms^{-1}, to 0.5 when $k_r = 10^3$ ms^{-1}.

We next analyzed the number of electron-hole pairs in a QD under steady-state conditions. Figure 3(d) shows the probability of finding single or multiple e-h pairs for different generation rates. For very low generation rates ($\leqslant$1 ms^{-1}), radiative recombination is dominant and the probability of finding an e-h pair is low. As the generation rate increases, the probability of finding multiple e-h pairs increases progressively and QY_{on} decreases [see Fig. 3(c)]. This effect was reported by Kraus et al.[26] who showed that the photoluminescence intensity did not increase proportionally with increasing generation rate for CdSe/ZnS QDs.

C. Pulsed laser excitation

Experimentally, intensity-time curves are usually obtained under continuous excitation where $k_r > g$. However, in some cases pulsed laser excitation is used to study blinking.[15,16,26] In these experiments, the laser pulse is typically on the order of picoseconds or less, much faster than other processes such as radiative recombination and Auger recombination, and the repetition time is typically on the order of microseconds. In these experiments, multiple e-h pairs can be generated in each pulse before any relaxation process can occur. The generation of multiple e-h pairs in a single pulse ($N_p \geqslant 2$) results in the instantaneous population of states where Auger recombination is significant. As long as $k_A > k_r$, all additional electron-hole pairs in a pulse will recombine very quickly, and

the quantum yield in the on state is decreased; however, the blinking behavior is unchanged. When $k_A \approx k_r$, the additional e-h pairs can undergo radiative recombination and hence the on intensity will be higher than for continuous excitation with the same repetition time, even though the quantum yield for the pulsed experiment will be lower.

D. Distributions of on and off times

With fixed values of k_t and k_d, the distributions of on and off times are exponential [$f = A\exp(-\tau/\tau_0)$]. For example, Figure 4(b) shows an intensity-time curve and the distributions of on and off times for $k_t = 10^0$ ms^{-1} and $k_d = 10^{-3}$ ms^{-1} ($k_{nrt} = 0$). The distributions are exponential with $\tau_{0,on} = 1.14 \pm 0.04$ s and $\tau_{0,off} = 1.17 \pm 0.08$ s ($P_{on} = 0.49 \pm 0.01$).

An exponential distribution of on and off times is expected for constant trapping and detrapping rates[33] as pointed out by Efros and Rosen,[2] and has been observed experimentally for quantum jumps in atomic systems.[34] In practice, the distribution of on and off times obtained from analysis of intensity-time curves for QDs usually exhibits power-law behavior ($f = B\tau^{-\alpha}$), with exponents α typically between 1.0 and 2.0.[29,30,35,36]

Figure 4(c) shows the distribution of on and off times for a linear distribution of k_t and k_d,[3] where k_t varies from 10^{-2} to 10^2 ms^{-1} and k_d varies from 10^{-5} to 10^{-1} ms^{-1} [see Fig. 4(a)]. For each trapping (detrapping) event the trapping (detrapping) rate constant is selected randomly over the given range, where all rate constants have equal probability. The distributions show power-law behavior with $\alpha_{on} = 1.86 \pm 0.06$ and $\alpha_{off} = 1.86 \pm 0.03$ ($P_{on} = 0.52 \pm 0.05$).

The power-law exponent is dependent on the function that describes the distribution of trapping and detrapping rate constants. For example, a parabolic distribution [Fig. 4(d)] of k_t and k_d (over the same range), results in power-law distributions with $\alpha_{on} = 1.37 \pm 0.06$ and $\alpha_{off} = 1.35 \pm 0.06$ ($P_{on} = 0.42 \pm 0.14$). An exponential distribution [Fig. 4(e)] of k_t and k_d results in power-law distributions with $\alpha_{on} = 0.98 \pm 0.06$ and $\alpha_{off} = 1.02 \pm 0.06$ ($P_{on} = 0.52 \pm 0.15$).

To describe the influence of variable trapping and detrapping rate constants on the distribution of on and off times, it is convenient to refer to the effective trapping and detrapping rates ($r_{t,eff}$ and $r_{d,eff}$). The range of trapping and detrapping rate constants gives rise to a range of $r_{t,eff}$ and $r_{d,eff}$. Power-law behavior is only observed when there is a distribution of effective trapping and detrapping rates where $\tau_{t,eff}$ ($1/r_{t,eff}$) and $\tau_{d,eff}$ ($1/r_{d,eff}$) span a range from τ_{bin} to $\sim$0.1τ_{total}. For a typical bin time of 10 ms and a typical total time of 1000 s, this corresponds to a range of about four orders of magnitude. The influence of the distribution of trapping and detrapping rate constants on the power-law exponent is simply related to the distribution of trapping and detrapping events. For example, a parabolic distribution has more events at longer times than a linear distribution which results in more probability density at longer times and hence a smaller slope. Thus the range of power-law exponents observed experimentally can be obtained simply by tuning the function that describes the range of trapping and detrapping rate constants.

Physically, a distribution in values of k_t and k_d is easily justified. For example, if trapping involves tunneling to trap
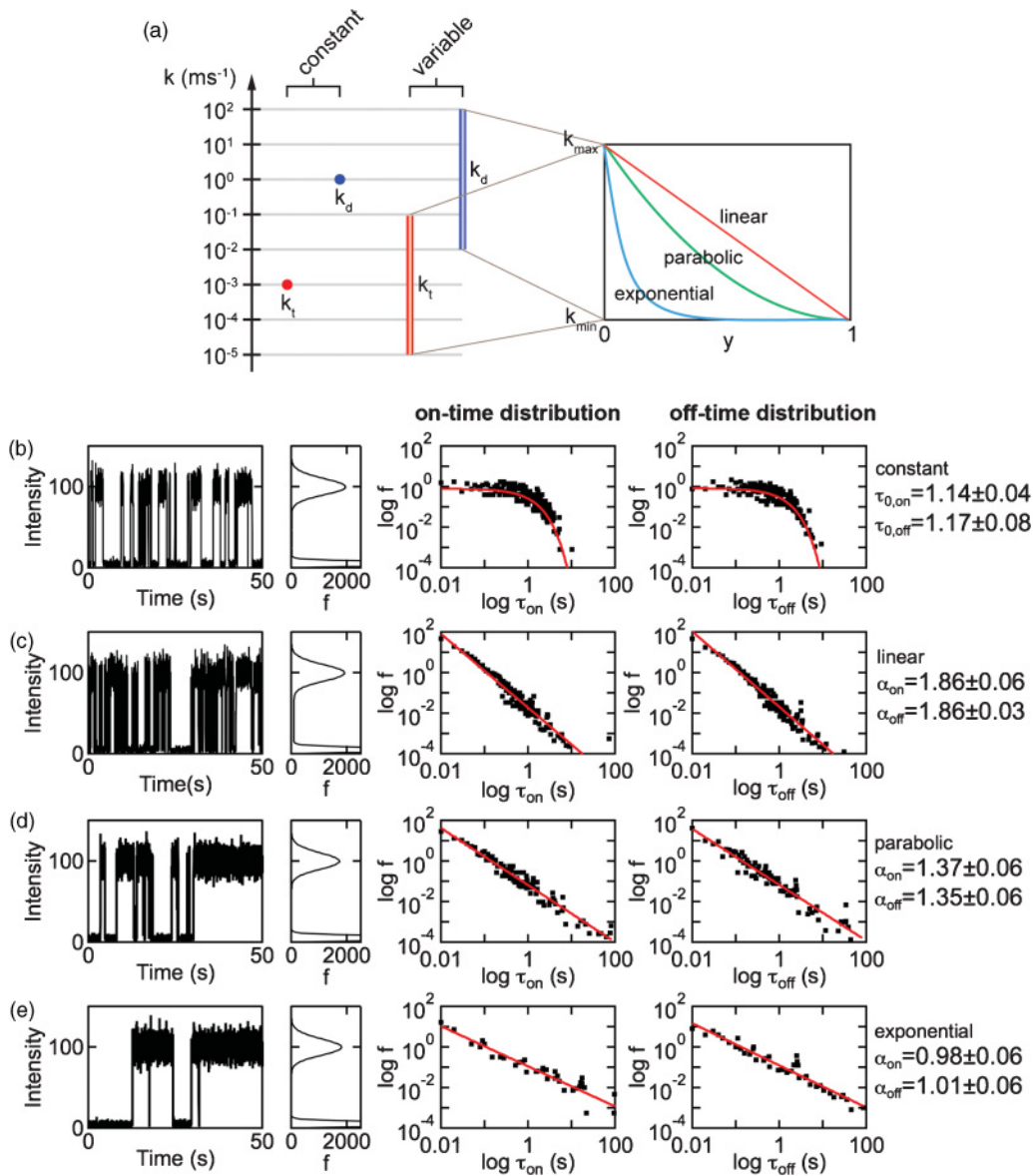
FIG. 4. (Color) Simulated intensity-time curves, intensity distributions, and distributions of on and off times for QD excitation for constant and variable trapping and detrapping rate constants (k_t and k_d) with $k_{nrt} = 0$ ms^{-1}, $s = 10$, $k_r = 10^5$ ms^{-1}, $k_A = 10^7$ ms^{-1}, and $g = 10$ ms^{-1}. (a) The range and distribution of trapping and detrapping rate constants. (b) Constant trapping and detrapping rate constants: $k_t = 10^0$ ms^{-1}, $k_d = 10^{-3}$ ms^{-1}. (c) Linear distribution of trapping and detrapping rate constants: $k_t = 10^{-2}$–10^2 ms^{-1}, $k_d = 10^{-5}$–10^{-1} ms^{-1}. (d) Parabolic distribution of trapping and detrapping rate constants: $k_t = 10^{-2}$–10^2 ms^{-1}, $k_d = 10^{-5}$–10^{-1} ms^{-1}. (e) Exponential distribution of trapping and detrapping rate constants: $k_t = 10^{-2}$–10^2 ms^{-1}, $k_d = 10^{-5}$–10^{-1} ms^{-1}. For details of the variable trapping and detrapping rates, see Supplemental Material.[3] The exponential constant $\tau_{0,on/off}$ and power-law exponents $\alpha_{on/off}$ were obtained from 10 simulations.

states in the shell, then a distribution of distances from the QD core would be expected to give rise to a distribution in trapping and detrapping rates. Similarly, a distribution in the energy of traps at the core-shell interface would also be expected to give a distribution of trapping and detrapping rates.

*Author to whom correspondence should be addressed: searson@jhu.edu

[1]P. Frantsuzov, M. Kuno, B. Janko, and R. A. Marcus, Nature Physics **4**, 519 (2008).

[2]A. L. Efros and M. Rosen, Phys. Rev. Lett. **78**, 1110 (1997).

[3]See Supplemental Material at http://link.aps.org/supplemental/10.1103/PhysRevB.84.125317 for details.

[4]M. Kuno, D. P. Fromm, S. T. Johnson, A. Gallagher, and D. J. Nesbitt, Phys. Rev. B **67**, 125304 (2003).

[5]G. Margolin and E. Barkai, J. Chem. Phys. **121**, 1566 (2004).

[6]R. Verberk, A. M. van Oijen, and M. Orrit, Phys. Rev. B **66**, 233202 (2002).

[7]T. D. Krauss and J. J. Peterson, J. Phys. Chem. Lett. **1**, 1377 (2010).

[8]F. Cichos, C. von Borczyskowski, and M. Orrit, Curr. Opin. Colloid Interface Sci. **12**, 272 (2007).

[9]K. A. Fichthorn and W. H. Weinberg, J. Chem. Phys. **95**, 1090 (1991).

[10]L. Brus, J. Phys. Chem. **90**, 2555 (1986).

[11]L. E. Brus, J. Chem. Phys. **80**, 4403 (1984).

[12]A. J. Nozik, M. C. Beard, J. M. Luther, M. Law, R. J. Ellingson, and J. C. Johnson, Chem. Rev. **110**, 6873 (2010).

[13]T. K. Gupta and J. Doh, J. Mater. Res. **7**, 1243 (1992).

[14]P. Spinicelli, S. Buil, X. Quelin, B. Mahler, B. Dubertret, and J. P. Hermier, Phys. Rev. Lett. **102**, 136801 (2009).

[15]J. J. Peterson and D. J. Nesbitt, Nano Lett. **9**, 338 (2009).

[16]K. Goushi, T. Yamada, and A. Otomo, J. Phys. Chem. C **113**, 20161 (2009).

[17]P. Michler, A. Imamoglu, M. D. Mason, P. J. Carson, G. F. Strouse, and S. K. Buratto, Nature **406**, 968 (2000).

[18]S. A. Crooker, J. A. Hollingsworth, S. Tretiak, and V. I. Klimov, Phys. Rev. Lett. **89**, 186802 (2002).

[19]X. Y. Wang, X. F. Ren, K. Kahen, M. A. Hahn, M. Rajeswaran, S. Maccagnano-Zacher, J. Silcox, G. E. Cragg, A. L. Efros, and T. D. Krauss, Nature **459**, 686 (2009).

[20]V. Fomenko and D. J. Nesbitt, Nano Lett. **8**, 287 (2008).

[21]B. Mahler, P. Spinicelli, S. Buil, X. Quelin, J. P. Hermier, and B. Dubertret, Nat. Mater. **7**, 659 (2008).

[22]P. T. Landsberg, Phys. Status Solidi **41**, 457 (1970).

[23]L. W. Wang, M. Califano, A. Zunger, and A. Franceschetti, Phys. Rev. Lett. **91**, 056404 (2003).

[24]V. I. Klimov, A. A. Mikhailovsky, D. W. McBranch, C. A. Leatherdale, and M. G. Bawendi, Science **287**, 1011 (2000).

[25]P. P. Jha and P. Guyot-Sionnest, Acs Nano **3**, 1011 (2009).

[26]R. M. Kraus, P. G. Lagoudakis, J. Muller, A. L. Rogach, J. M. Lupton, J. Feldmann, D. V. Talapin, and H. Weller, J. Phys. Chem. B **109**, 18214 (2005).

[27]A. Haug, J. Phys. C-Solid State Physics **16**, 4159 (1983).

[28]W. Shockley and W. T. Read, Phys. Rev. **87**, 835 (1952).

[29]M. Kuno, D. P. Fromm, H. F. Hamann, A. Gallagher, and D. J. Nesbitt, J. Chem. Phys. **115**, 1028 (2001).

[30]C. H. Crouch, O. Sauter, X. H. Wu, R. Purcell, C. Querner, M. Drndic, and M. Pelton, Nano Lett. **10**, 1692 (2010).

[31]J. Zhao, G. Nair, B. R. Fisher, and M. G. Bawendi, Phys. Rev. Lett. **104**, 157403 (2010).

[32]H. Htoon, A. V. Malko, D. Bussian, J. Vela, Y. Chen, J. A. Hollingsworth, and V. I. Klimov, Nano Lett. **10**, 2401 (2010).

[33]R. J. Cook and H. J. Kimble, Phys. Rev. Lett. **54**, 1023 (1985).

[34]R. Blatt and P. Zoller, Eur. J. Phys. **9**, 250 (1988).

[35]M. Kuno, D. P. Fromm, H. F. Hamann, A. Gallagher, and D. J. Nesbitt, J. Chem. Phys. **112**, 3117 (2000).

[36]S. Hohng and T. Ha, J. Am. Chem. Soc. **126**, 1324 (2004).